Journal of Visualized Experiments

Machine Learning Algorithms for Early Detection of Bone Metastases in an Experimental Rat Model

--Manuscript Draft--

Article Type:	Invited Methods Article - JoVE Produced Video
Manuscript Number:	JoVE61235R2
Full Title:	Machine Learning Algorithms for Early Detection of Bone Metastases in an Experimental Rat Model
Section/Category:	JoVE Cancer Research
Keywords:	Machine learning; neural networks; bone metastases; disseminated tumor cells; breast neoplasms; multiparametric imaging
Corresponding Author:	Tobias Bäuerle Universitatsklinikum Erlangen Erlangen, Bavaria GERMANY
Corresponding Author's Institution:	Universitatsklinikum Erlangen
Corresponding Author E-Mail:	tobias.baeuerle@uk-erlangen.de
Order of Authors:	Stephan Ellmann
	Lisa Seyler
	Clarissa Gillmann
	Vanessa Popp
	Christoph Treutlein
	Aline Bozec
	Michael Uder
	Tobias Bäuerle
Additional Information:	
Question	**Response**
Please indicate whether this article will be Standard Access or Open Access.	Standard Access (US$2,400)
Please indicate the **city, state/province, and country** where this article will be **filmed**. Please do not use abbreviations.	Erlangen, Bavaria, GERMANY

Department of Radiology Maximiliansplatz 3 91054 Erlangen, Germany

Department of Radiology
Head: Prof. Dr. med. Michael Uder

91054 Erlangen, Maximiliansplatz 3, Germany
Phone: +49-9131 85-45521
Fax: +49-9131 85-36068
Email: tobias.baeuerle@uk-erlangen.de

Journal of Visualized Experiments (JoVE)
Editorial Office
1 Alewife Center Suite 200 Cambridge MA 02140

Elizabeth Heppenheimer, Ph.D.

Erlangen, 2020/03/09

Manuscript Revision: JoVE61235-R1

Dear Dr. Heppenheimer,

Thank you very much for providing us with another review of our manuscript (JoVE61235-R1). Based on the comments by the Editorial Office, we have addressed all issues and adapted our manuscript accordingly.

Please find the revised manuscript attached. All changes have been tracked using the respective MS Word function.

As requested, we managed to cut the yellow-highlighted parts down to less than 2.75 pages by deleting all the code from the manuscript. In the respective steps of the protocol, we now refer to the provided script files instead.

We hope that our revised manuscript meets your requirements for publication in JoVE.

Yours sincerely,

Tobias Bäuerle, MD
Corresponding author

Stephan Ellmann, MD
First author

TITLE:

Machine Learning Algorithms for Early Detection of Bone Metastases in an Experimental Rat Model

AUTHORS AND AFFILIATIONS:

Stephan Ellmann[1], Lisa Seyler[1], Clarissa Gillmann[2], Vanessa Popp[1], Christoph Treutlein[1], Aline Bozec[3], Michael Uder[1], Tobias Bäuerle[1]

[1]Department of Radiology, University Hospital Erlangen, Friedrich-Alexander-Universität Erlangen-Nürnberg, Erlangen, Germany
[2]Department of Medical Physics in Radiation Oncology, German Cancer Research Center, Heidelberg, Germany
[3]Department of Internal Medicine 3, University Hospital Erlangen, Friedrich-Alexander-Universität Erlangen-Nürnberg, Erlangen, Germany

Corresponding Author:

Tobias Bäuerle, MD (Tobias.Baeuerle@uk-erlangen.de)

Email Addresses of Co-authors:

Stephan Ellmann (Stephan.Ellmann@uk-erlangen.de)
Lisa Seyler (Lisa.Seyler@uk-erlangen.de)
Clarissa Gillmann (C.Gillmann@dkfz.de)
Vanessa Popp (Vanessa.Popp@uk-erlangen.de)
Christoph Treutlein (Christoph.Treutlein@uk-erlangen.de)
Aline Bozec (Aline.Bozec@uk-erlangen.de)
Michael Uder (Michael.Uder@uk-erlangen.de)

KEYWORDS:

machine learning, neural networks, bone metastases, disseminated tumor cells, breast neoplasms, multiparametric imaging

SUMMARY:

This protocol was designed to train a machine learning algorithm to use a combination of imaging parameters derived from magnetic resonance imaging (MRI) and positron emission tomography/computed tomography (PET/CT) in a rat model of breast cancer bone metastases to detect early metastatic disease and predict subsequent progression to macrometastases.

ABSTRACT:

Machine learning (ML) algorithms permit the integration of different features into a model to perform classification or regression tasks with an accuracy exceeding its constituents. This protocol describes the development of an ML algorithm to predict the growth of breast cancer bone macrometastases in a rat model before any abnormalities are observable with standard imaging methods. Such an algorithm can facilitate the detection of early metastatic disease (i.e., micrometastasis) that is regularly missed during staging examinations.

The applied metastasis model is site-specific, meaning that the rats develop metastases exclusively in their right hind leg. The model's tumor-take rate is 60%–80%, with macrometastases becoming visible in magnetic resonance imaging (MRI) and positron emission tomography/computed tomography (PET/CT) in a subset of animals 30 days after induction, whereas a second subset of animals exhibit no tumor growth.

Starting from image examinations acquired at an earlier time point, this protocol describes the extraction of features that indicate tissue vascularization detected by MRI, glucose metabolism by PET/CT, and the subsequent determination of the most relevant features for the prediction of macrometastatic disease. These features are then fed into a model-averaged neural network (avNNet) to classify the animals into one of two groups: one that will develop metastases and the other that will not develop any tumors. The protocol also describes the calculation of standard diagnostic parameters, such as overall accuracy, sensitivity, specificity, negative/positive predictive values, likelihood ratios, and the development of a receiver operating characteristic. An advantage of the proposed protocol is its flexibility, as it can be easily adapted to train a plethora of different ML algorithms with adjustable combinations of an unlimited number of features. Moreover, it can be used to analyze different problems in oncology, infection, and inflammation.

INTRODUCTION:

The purpose of this protocol is to integrate several functional imaging parameters from MRI and PET/CT into a model-averaged neural network (avNNet) ML algorithm. This algorithm predicts the growth of macrometastases in a rat model of breast cancer bone metastases at an early timepoint, when macroscopic changes within the bone are not yet visible.

Prior to the growth of macrometastases, a bone marrow invasion of disseminated tumor cells occurs, commonly referred to as micrometastatic disease[1,2]. This initial invasion can be considered an early step in metastatic disease, but is typically missed during conventional staging examinations[3,4]. Although the currently available imaging modalities cannot detect bone marrow microinvasion when used alone, a combination of imaging parameters yielding information on vascularization and metabolic activity has been shown to perform better[5]. This complementary benefit is achieved by combining different imaging parameters into an avNNet, which is an ML algorithm. Such an avNNet allows for the reliable prediction of bone macrometastases formation before any visible metastases are present. Therefore, integrating imaging biomarkers into an avNNet could serve as a surrogate parameter for bone marrow microinvasion and early metastatic disease.

To develop the protocol, a previously described model of breast cancer bone metastases in nude rats was used[6–8]. The advantage of this model is its site-specificity, meaning that the animals develop bony metastases exclusively in their right hind leg. However, the tumor-take rate of this approach is 60%–80%, so a considerable number of the animals do not develop any metastases during the study. Using imaging modalities such as MRI and PET/CT, the presence of metastases is detectable from day 30 postinjection (PI). At earlier time points (e.g., 10 PI) imaging does not

distinguish between animals that will develop metastatic disease and those will not (**Figure 1**).

An avNNet trained on functional imaging parameters acquired on day 10 PI, as described in the following protocol, reliably predicts or excludes the growth of macrometastases within the following ~3 weeks. Neural Networks combine artificial nodes within different layers. In the study protocol, the functional imaging parameters for bone marrow blood supply and metabolic activity represent the bottom layer, while the prediction of malignancy represents the top layer. An additional intermediate layer contains hidden nodes that are connected to both the top and the bottom layer. The strength of the connections between the different nodes is updated during the training of the network to perform the respective classification task with high accuracy[9]. The accuracy of such a neural network can be further increased by averaging the outputs of several models, resulting in an avNNet[10].

PROTOCOL:

All care and experimental procedures were performed in accordance with national and regional legislation on animal protection, and all animal procedures were approved by the State Government of Franconia, Germany (reference number 55.2 DMS-2532-2-228).

1. Induction of breast cancer bone metastases in the right hind leg of nude rats

NOTE: A detailed description of the induction of breast cancer bone metastases in nude rats has been published elsewhere[6,8]. The most relevant steps are presented below.

1.1. Culture MDA-MB-231 human breast cancer cells in RPMI-1640, supplemented with 10% fetal calf serum (FCS). Keep the cells under standard conditions (37 °C, 5% CO_2) and passage the cells 2–3 times a week.

1.2. Wash near-confluent MDA-MB-231 cells with 2 mM EDTA in phosphate-buffered saline (PBS), and then detach the cells with 0.25% trypsin. Determine the cell concentration with a Neubauer's chamber and resuspend them in 200 µL of RPMI-1640 at a concentration of 1.5 x 10^5 cells/200 µL.

1.3. Use 6–8 week-old nude rats and keep them under pathogen-free, controlled conditions (21 °C ± 2 °C room temperature, 60% humidity, and 12 h light-dark rhythm). Offer autoclaved feed and water ad libitum.

1.4. Before performing the surgery, inject an analgesic drug (e.g., Carprofen 4 mg/kg) subcutaneously. Anesthetize rats with an isoflurane (1–1.5 vol. %)/oxygen mixture at a flow rate of 2 L/min. Check the anesthetic depth by toe pinching.

1.5. For surgery, use an operating microscope with a 16x magnification.

1.6. Perform a 2–3 cm cut in the rat's right inguinal region. Dissect all arteries in the right inguinal

region, including the femoral artery (FA), the superficial epigastric artery (SEA), the descending genicular artery (DGA), the popliteal artery (PA), and the saphenous artery (SA). Place two removable clips on the FA: one proximal to the beginning of the SEA, and another directly proximal to the beginning of the DGA.

1.7. Ligate the distal portion of the SEA. Perform a cut of the SEA's wall and insert a 0.3 mm diameter needle into the SEA. Connect a syringe containing the cell suspension from step 1.2 to the needle. Remove the distal clip from the FA and clip the SA instead.

1.8. Slowly inject the MDA-MB-231 cell suspension from step 1.2 (1.5×10^5 cells/200 µL) into the SEA. Remove the needle, ligate the SEA, and remove the artery clips. Close the wound using surgical clips and terminate anesthesia. Monitor the animals daily to assess tumor size and any evidence of pain.

2. Magnetic resonance imaging (MRI)

NOTE: For a detailed description of MRI procedures, please see Bäuerle et al.[11].

2.1. Perform MRI 10 days PI using a dedicated experimental scanner (see **Table of Materials**) or a human MR system with an appropriate animal coil.

2.2. Anesthetize the rat with an isoflurane (1–1.5 vol. %)/oxygen mixture as described above. Place a catheter in the rat's tail vein and tape it to the tail. Connect a syringe containing the contrast agent (0.1 mmol/kg Gd-DTPA in approximately 0.5 mL).

2.3. Place the anesthetized rat in the MR system. Locate the distal femur and proximal tibia of the right hind leg in an anatomic sequence (e.g., T2-weighted turbo spin echo sequence; TR = 8,654 ms; TE = 37 ms; matrix 320 x 272; FOV = 65 mm x 55 mm; slice thickness = 1 mm; scan time 11:24 min).

2.4. Determine the slices covering the distal femur and proximal tibia of the right hind leg and start the DCE-MRI sequence (e.g., fast low angle shot sequence; TR = 3.9 ms; TE = 0.88 ms; matrix = 256 x 216; FOV = 65 x 54 mm^2; slice thickness = 1 mm; 8 slices; 100 time points; scan time = 8:25 min). After 30 s, start injecting the contrast agent over a time period of 10 s.

NOTE: The total time to perform an MRI examination is approximately 20 min per animal.

3. Positron emission tomography/computed tomography (PET/CT)

NOTE: For a detailed description of the PET procedures, please see Cheng at al.[12].

3.1. Perform PET/CT imaging 10 days PI using a dedicated experimental scanner (see **Table of Materials**).

3.2. Keep the animals fasted prior to imaging. Anesthetize the rat as described in step 2.2 and insert a catheter in the tail vein as described above.

3.3. Inject 6 MBq of ^{18}F-Fluorodeoxyglucose (^{18}F-FDG) into the tail vein and wait ~30 min to allow the tracer to distribute properly.

3.4. Perform a CT acquisition (tube voltage = 80 kV, tube current = 500 µA, isotropic resolution = 48.9 µm, duration = 10 min).

3.5. Perform a static PET acquisition (lower/upper discriminatory level = 350/650 keV; timing window = 3.438 ns; duration = 15 min).

4. Alternative imaging strategies

4.1. For an early assessment of MDA-MB-231 cells in the hind leg, inoculate 1.5 x 10^5 labeled cells /200 µL for bioluminescence (i.e., cells expressing luciferin, MDA-MB-231-LUC[13]) or fluorescence imaging (i.e., cells expressing green or red fluorescent protein, MDA-MB-231-GFP/RFP[13]). Use the system for preclinical optical imaging to detect intraosseous MDA-MB-231 cells after tumor cell inoculation[14].

4.2. Perform experimental ultrasound using a dedicated scanner after intravenous injection of microbubbles to derive morphological and functional parameters of vascularization comparable to MRI[7].

5. MRI analysis

5.1. Use a DICOM viewer[15] with a DCE Plugin[16] and load the DCE sequence in 4D-mode by clicking the "**Import**" button in the top menu, selecting the DICOM folder containing the MR images from step 2.4, and clicking "**4D Viewer**" in the top menu.

5.2. Place a circular 2-dimensional region of interest (ROI), with a target size of 1.5 mm^2, in the proximal tibial shaft's bone marrow of the right hind leg, preferably using image numbers 4 or 5 from the sequence consisting of 8 images, as these center images provide more stable results.

5.3. Start the DCE plugin from the top menu, select "**Relative Enhancement**" in the "**Plot Type**" field, and define the baseline range from time points 1 to 5 by typing these numbers into the respective fields. Export the analysis as a .txt file with the respective button and choose "DCEraw.txt" as the file name.

5.4. Open RStudio[17] and load the provided DCE-Script.R file via the "**File**" menu by selecting "**Open File**". Run the entire script by selecting "**Code**", then "**Run Region**" and then "**Run All**" from the menu. Copy the output to the provided template file named "ImagingFeatures.xlsx" (**Figure 2**).

5.5. In the DICOM viewer, place a second ROI within the back muscle of the animal and repeat steps 5.2–5.4 to obtain the muscle DCE measurements for normalization purposes. Within the spreadsheet "ImagingFeatures.xlsx", the respective bone measurements are automatically divided by the respective muscle measurements for normalization purposes.

5.6. Repeat steps 5.1–5.5 for all animals and complete the spreadsheet.

6. PET/CT analysis

6.1. Open the PET/CT analysis software and import the data obtained in step 3 by clicking "**File**", followed by "**Manual import**". Mark the ct.img.hd and the pet.img.hdr files. Click "**Open**" and select "**Import all**".

6.2. Open the datasets by selecting "**General analysis**", followed by "**OK**".

6.3. Select "**ROI Quantification**", followed by "**Create**", and then "**Create a ROI from a template**". Place a 2-dimensional ROI approximately 4 mm x 6 mm into the proximal tibial shaft's bone marrow of the right hind leg.

6.4. Select "**ROIs (Target 1 overlay)**" and write down mean, minimum, and maximum values in Bq/mL.

6.5. Calculate the maximum standardized uptake value (SUV_{max}): Divide the maximum value (Bq/mL) by the injected activity and multiply the result by the weight of the animal in grams. Enter the result into the spreadsheet (**Figure 2**).

7. Determining the tumor-take rate

7.1. To diagnose tumor growth in the right hind leg, repeat MR and PET/CT imaging on day 30 PI, as described above.

NOTE: Tumors will be clearly visible on day 30 PI and feature T2w-hyperintense lesions and clear contrast enhancement in MRI, along with a clearly elevated SUV_{max} in PET/CT. According to previous experiments, 60%–80% of the animals will develop metastases in their right hind leg.

7.2. Complete the spreadsheet by adding an additional "Tumor" column and enter "1" for every animal that presents metastases, and "0" for every animal without visible tumor burden (**Figure 2**). Save the spreadsheet as "ImagingFeatures.xlsx" within the Downloads folder.

8. Feature selection

8.1. To determine the most relevant features for prediction of future tumor growth, import the spreadsheet into an open-source data visualization, machine learning, and data mining toolkit[18].

8.2. Draw the **File-subroutine** from the **Data menu** into the workspace on the right and double-click it. Load the spreadsheet by clicking the "**Folder**" icon and selecting the file "ImagingFeatures.xlsx". Select the **"Export**" worksheet and assign the target-attribute to the variable "**Tumor**". Assign the "**Skip**" function to the animal number (**Figure 3**).

8.3. Draw the "**Rank**" subroutine from the **Data menu** into the workspace and connect the "**File**" and "**Rank**" subroutines by drawing a line between them.

8.4. Open the "**Rank**" subroutine by double-clicking on its icon, and select the "**Information Gain**" algorithm[19].

8.5. From the five acquired parameters, use the top three for further analyses (SUV_{max}, PE, and AUC).

Note: These parameters reflect metabolic activity (SUV_{max}) and tissue vascularization (PE and AUC).

9. ML analysis

9.1. Open RStudio 3.4.1[17] and load the provided TrainModel.R-Script via the "**File**" menu.

9.2. Install the required libraries (this only has to be done once) by typing:
install.packages(c("caret", "readxl", "pROC", "RcmdrPlugin.EZR", "ggplot2"))

9.3. To load the required libraries and set the Downloads folder as the working directory, select the lines 3–5 within the TrainModel.R Script.

9.4. Run the selected code by clicking "**Code**" within the menu, and then "**Run Selected Line(s)**".

10. Training an avNNet ML algorithm

10.1. To train an avNNet algorithm, select the lines 8–39 from the TrainModel.R-Script (see step 9.1).

10.2. Run the selected code by clicking "**Code**" within the menu, and then "**Run Selected Line(s)**".

11. Analyzing the ML algorithm's results

11.1. To assess standard parameters of diagnostic accuracy (sensitivity, specificity, positive and negative predictive values, and likelihood ratios), select the lines 41–50 from the TrainModel.R-Script.

11.2. Run the selected code by clicking "**Code**" within the menu, and then "**Run Selected Line(s)**".

12. Comparing the final model's Receiver Operating Characteristic (ROC) curve with the ROC curves of its constituent parameters

12.1. To perform DeLong's tests to compare the model's ROC curve with the ROC curves of its constituent parameters, select the lines 52–62 from the TrainModel.R-Script (see step 9.1).

12.2. Run the selected code by clicking "**Code**" within the menu, and then "**Run Selected Line(s)**".

REPRESENTATIVE RESULTS:

The rats recovered quickly from the surgery and injection of the MDA-MB-231 breast cancer cells and were then subjected to MR- and PET/CT imaging on days 10 and 30 PI (**Figure 1**). A representative DCE analysis of a rat's right proximal tibia is presented in **Figure 2A**. The DCE raw measurements were saved by selecting the "**Export**" button and choosing "DCEraw.txt" as the file name.

Subsequent calculations of the dynamic parameters, AUC, PE, and washout were performed in RStudio with the respective script. The output of the DCE measurements had to be saved as "DCEraw.txt" within the "Downloads" folder, so that the script could be run directly without additional configurations to provide a data table, as depicted in **Figure 2B**. These data were copied to the provided spreadsheet (**Figure 2C**). Similarly, the DCE parameters for muscular tissue were determined and transferred to the spreadsheet (**Figure 2D**,**E**). These values were normalized by dividing the bone measurements by the muscle measurements; this was performed automatically within the spreadsheet. From the PET/CT, the calculated SUV_{max} values were subsequently transferred into the table (**Figure 2F**).

On day 30 PI, all animals were evaluated to determine whether or not they developed metastases, and the table was completed by coding positive tumor burden as "1" and healthy animals as "0" within the rightmost column of the spreadsheet (**Figure 2C**).

The spreadsheet was imported into the open-source data visualization, machine learning, and data mining toolkit, and feature ranking revealed the SUV_{max}, PE, and AUC as the top three features for prediction of metastatic disease (**Figure 3**). These parameters reflect metabolic activity (SUV_{max}) and tissue vascularization (PE and AUC).

Running the TrainModel.R Script automatically imported the spreadsheet and calculated an avNNet. The optimal hyperparameter combination was determined (**Figure 4A**) and the final model was then calculated using the optimal hyperparameter combination (**Figure 4B**). Subsequently, a set of standard diagnostic parameters was calculated (**Figure 4C**) and an ROC curve of the model was plotted (**Figure 4D**).

The positive result is shown in **Figure 4B–D**. A comparison of the model's ROC curve with the ROC curve of its three constituents (i.e., AUC, PE, and SUV_{max}) revealed that the model performed significantly better than all of its three constituents ($p = 0.01$ for AUC, $p = 0.003$ for PE, and $p = 0.007$ for SUV_{max}). The combination of the three selected parameters to an avNNet was more

sensitive, thus allowing prediction of macroscopic disease with an overall accuracy of 85.7% (95% confidence interval = 67.3%–96.0%). These results were obtained from an analysis of 28 samples. The confidence intervals can be further narrowed by increasing the number of animals.

The negative results could be obtained as described here. The accuracy measures were highly sensitive to specific types of machine learning algorithms and to steps of data preprocessing. Neural Networks, in particular, tended to perform better when the input data were normalized. This was achieved by the "BoxCox" function in section 10 of the protocol (lines 22 and 36 within the provided TrainModel.R-Script). Refraining from normalization and using a different algorithm (e.g., a neural network not averaged), by changing the method to "nnet" (lines 21 and 35 within the provided TrainModel.R-Script), resulted in an area of 0.594 under the ROC curve (**Supplementary Figure 1**). Such a model failed to outperform its three constituents significantly (all $p > 0.15$).

Because the script was optimized for RStudio 3.4.1 and the caret package version 6.0-84, using different software versions might yield different results. Running the provided scripts with the software versions used in this manuscript will give similar results. However, if readers aim to modify the script, add additional variables, change document folders or file names, or modify the machine learning algorithms in greater detail, respective adjustments of the code will be necessary. For these cases, the manual of the caret-package offers in-depth explanations[20].

FIGURE AND TABLE LEGENDS:

Figure 1: Representative MR and PET/CT images. MR and PET/CT images of the right hind leg of an animal that did not develop metastases over the course of the study (two leftmost columns, with images from day 10 and day 30 PI), and an animal that developed metastases between day 10 and day 30 PI (two rightmost columns, metastases marked with arrows). Note the high signal intensity of metastases in the T2w images (upper row), the contrast enhancement depicted by the increased area under the curve (AUC; second row), and the increased maximum standardized uptake value in the PET/CT (SUV_{max}; third row). Note that there are no visible differences in the images acquired on day 10 PI (first and third column) between the animal with metastases on day 30 PI and the animal that developed no bone metastases. This figure was modified from Ellmann et al.[5].

Figure 2: Assessment of the imaging features and compilation into a spreadsheet. (**A**) The dynamic contrast enhancement of the proximal tibia's bone marrow was analyzed with a freeware DICOM viewer[15] using a DCE plugin[16]. The respective measurements were saved, and (**B**) further analyzed with the provided DCE-Script.R-file in RStudio[17]. (**C**) The output was copied into a spreadsheet (see supplementary material for a template). (**D**) Likewise, the DCE measurement was performed for adjacent muscular tissue, analyzed using RStudio (**E**), and then copied to the spreadsheet. Data were normalized by dividing the results of the bone measurements by the results of the muscle measurements (**C**; salmon-shaded cells). (**F**) The PET/CT measurements were performed with the vendor's software. The maximum standardized uptake value was calculated by dividing the respective measurement by the injected activity and multiplying it by the animal's body weight. The result was subsequently copied into the

spreadsheet.

Figure 3: Feature ranking. Ranking of the acquired imaging features was performed within an open-source data visualization, machine learning, and data mining toolkit[18] by importing the spreadsheet via the "File"-subroutine, and analyzing it via the "Rank"-subroutine.

Figure 4: Representative RStudio output. The machine learning algorithm was developed using RStudio[17] with the provided TrainModel.R-Script file. (**A**) A grid search among different hyperparameter combinations for the model-averaged neural network revealed a size of three neurons and a decay of 0.0005 as an optimum. (**B**) Using this hyperparameter combination, a full network was trained and cross-validated, reaching an overall accuracy of 85.7%. (**C**) Standard parameters of diagnostic accuracy, including sensitivity, specificity, positive and negative predictive values, and likelihood ratios, were calculated from a confusion matrix. (**D**) A representative ROC plot of the cross-validated model revealed an area under the curve (AUC) of 0.917.

Supplementary Figure 1: Negative result. Changing the ML algorithm to a Neural Network without averaging and refraining from normalization of the input parameters led to a drop of the area under the curve of the ROC curve from 0.917 (**Figure 4D**) to 0.594.

Supplementary Figure 2: Alternative feature ranking. In contrast to the standard method depicted in **Figure 3**, a random variable was also introduced ("Random"; highlighted in blue), with its importance included in the ranking. This approach confirmed the applied selection of the variables SUV_{max}, PE, and AUC.

DISCUSSION:

ML algorithms are powerful tools used to integrate several predictive features into a combined model and obtain an accuracy that exceeds that of its separate constituents when used alone. Nonetheless, the actual result depends on several critical steps. First, the ML algorithm used is a crucial factor, because different ML algorithms yield different results. The algorithm used in this protocol is an avNNet, but other promising algorithms include Extreme Gradient Boosting[21] or Random Forests. The caret package[20] for RStudio provides a plethora of different algorithms (currently >175), and the proposed protocol is highly flexible in terms of switching from one algorithm to another by simply changing single lines of code (e.g., changing method = "avNNet" to method ="rf") and adapting the TunedGrid-settings to the respective ML algorithm. For details, see the caret github repository[22]. An excellent overview of different algorithms and their performance with respect to different classification problems was published by Fernández-Delgado et al.[23] and could serve as a starting point for other experiments.

Another crucial factor is the choice of relevant features to include in an ML algorithm. This protocol proposes the use of the filter method, "Information Gain"[19], to rank the available features in descending order and use the most relevant ones to train the avNNet. Filter methods are based only on general assumptions, such as correlation with the variable to predict, so researchers should preselect features independently of the classifier used[24,25]. Such methods are

particularly effective in computation time and robust to overfitting. However, the cutoff that separates relevant from irrelevant features is defined by the user, making it somewhat arbitrary. For the proposed protocol, the features with the top 75% information gain were used, corresponding to SUV_{max}, PE, and AUC. This selection, however, can be systematically strengthened by including a random variable that has no relationship to the target, calculating its information gain, and then comparing it to the information gain of the real features (**Supplementary Figure 2**). This slightly more sophisticated approach additionally confirmed the choice of the three abovementioned features as being the most relevant. Nonetheless, several different filter methods exist, along with other approaches that select features with respect to a particular classifier algorithm, such as feature extraction and wrapper methods. Different feature selection approaches may yield different results.

To ensure generalizability of the ML algorithm and further prevent overfitting, the proposed protocol applies leave-one-out cross-validation (LOOCV). The best approach, however, would be to randomly remove a subset from the entire data set, and treat it as a testing set. The ML algorithm is then trained on the remainder of the data (i.e., the training set) to subsequently predict the outcome of the testing set. However, this approach needs a sufficiently large data set. For smaller sample sizes, application of LOOCV is common because it provides an almost unbiased estimate of a model's true generalization ability[26]. In LOOCV, the first data point is removed from the data set, and the avNNet is trained with the retained data. Then, the outcome of the formerly withheld data point is predicted and saved. This process is repeated for all data points, so that finally each outcome is predicted with data that were not used for training the algorithm. Other validation approaches include x-fold cross-validations (most commonly 10-fold) and can be easily applied by changing the respective trainControl parameter within the code to method="CV".

From a quantitative point-of-view, medical images are typically evaluated in a very basic way, largely relying on measurements of size and shape of potentially suspicious lesions or areas[27,28]. However, the advantage of the Digital Imaging and Communications in Medicine (DICOM) standard is that it allows extraction of many features, referred to as radiomics. The term “radiomics“ was initially defined as the high-throughput extraction of large quantities of image features[29], but was subsequently extended to include the conversion of images to higher dimensional data[30]. However, the higher dimensional data are mainly used to identify correlations rather than causes[30]. The features described in this protocol fall in between classic radiological features, such as size and shape, and radiomics, as they resemble generally accepted parameters of vascularization and metabolic activity. This offers a potential causal relation to the microinvasion of disseminated tumor cells. If desired by the user, an extraction of radiomic features can be performed with different software packages[31].

The protocol provided is not restricted to a finite number of features. Thus, it can be used with large radiomics data sets. However, the abovementioned issue of feature selection becomes increasingly important with growing data sets. The presented protocol can also be transferred to different study settings, e.g., from the fields of oncology, infection, or inflammation[32].

ACKNOWLEDGMENTS:

This work was supported by the German Research Foundation (DFG, Collaborative Research Centre CRC 1181, subproject Z02; Priority Programme µBone, projects BA 4027/10-1 and BO 3811), including additional support for the scanning devices (INST 410/77-1 FUGG and INST 410/93-1 FUGG), and by the Emerging Fields Initiative (EFI) "Big Thera" of the Friedrich-Alexander-University Erlangen-Nürnberg.

DISCLOSURES:

The authors declare no conflict of interest. The funders had no role in the design of the study; in the collection, analyses, or interpretation of data; in the writing of the manuscript, or in the decision to publish the results.

REFERENCES:

1. D'Oronzo, S., Brown, J., Coleman, R. The role of biomarkers in the management of bone-homing malignancies. *Journal of Bone Oncology*. **9**, 1–9 (2017).
2. Ellmann, S., Beck, M., Kuwert, T., Uder, M., Bäuerle, T. Multimodal imaging of bone metastases: From preclinical to clinical applications. *Journal of Orthopaedic Translation*. **3** (4), 166–177 (2015).
3. Braun, S., Pantel, K. Clinical significance of occult metastatic cells in bone marrow of breast cancer patients. *The Oncologist*. **6** (2), 125–132 (2001).
4. Braun, S., Rosenberg, R., Thorban, S., Harbeck, N. Implications of occult metastatic cells for systemic cancer treatment in patients with breast or gastrointestinal cancer. *Seminars in surgical oncology*. **20** (4), 334–46 (2001).
5. Ellmann, S. et al. Prediction of early metastatic disease in experimental breast cancer bone metastasis by combining PET/CT and MRI parameters to a Model-Averaged Neural Network. *Bone*. **120**, 254–261 (2018).
6. Bäuerle, T., Komljenovic, D., Berger, M. R., Semmler, W. Multi-modal imaging of angiogenesis in a nude rat model of breast cancer bone metastasis using magnetic resonance imaging, volumetric computed tomography and ultrasound. *Journal of Visualized Experiments*. (66), e4178 (2012).
7. Merz, M., Komljenovic, D., Semmler, W., Bäuerle, T. Quantitative contrast-enhanced ultrasound for imaging antiangiogenic treatment response in experimental osteolytic breast cancer bone metastases. *Investigative Radiology*. **47** (7), 422–429 (2012).
8. Bäuerle, T. et al. Characterization of a rat model with site-specific bone metastasis induced by MDA-MB-231 breast cancer cells and its application to the effects of an antibody against bone sialoprotein. *International Journal of Cancer*. **115** (2), 177–186 (2005).
9. Patel, J., Goyal, R. Applications of Artificial Neural Networks in Medical Science. *Current Clinical Pharmacology*. **2** (3), 217–226 (2008).
10. Naftaly, U., Intrator, N., Horn, D. Optimal ensemble averaging of neural networks. *Network: Computation in Neural Systems*. **8** (3), 283–296 (1997).
11. Bäuerle, T., Merz, M., Komljenovic, D., Zwick, S., Semmler, W. Drug-induced vessel remodeling in bone metastases as assessed by dynamic contrast enhanced magnetic resonance imaging and vessel size imaging: A longitudinal in vivo study. *Clinical Cancer Research*. **16** (12), 3215–3225 (2010).

12. Cheng, C. et al. Evaluation of treatment response of cilengitide in an experimental model of breast cancer bone metastasis using dynamic PET with 18F-FDG. *Hellenic Journal of Nuclear Medicine*. **14** (1), 15–20 (2011).
13. Marturano-Kruik, A. et al. Human bone perivascular niche-on-a-chip for studying metastatic colonization. *Proceedings of the National Academy of Sciences of the United States of America*. **115** (6), 1256–1261 (2018).
14. Sonntag, E. et al. In vivo proof-of-concept for two experimental antiviral drugs, both directed to cellular targets, using a murine cytomegalovirus model. *Antiviral Research*. **161**, 63–69 (2019).
15. Horos - Free DICOM Medical Image Viewer | Open-Source. at <https://www.horosproject.org/> (2015).
16. Sung, K. DCE Tool Plugin. at <http://kyungs.bol.ucla.edu/software/DCE_tool/DCE_tool.html>.
17. RStudio Team RStudio: Integrated Development for R. at <https://rstudio.com> (2015).
18. Demšar, J. et al. Orange: Data Mining Toolbox in Python. *Journal of Machine Learning Research*. **14**, 2349−2353 (2013).
19. Saeys, Y., Inza, I., Larrañaga, P. A review of feature selection techniques in bioinformatics. *Bioinformatics*. **23** (19), 2507–2517 (2007).
20. Kuhn, M. CRAN - Package caret. at <https://cran.r-project.org/web/packages/caret/index.html> (2016).
21. Chen, T. et al. CRAN: Package xgboost - Extreme Gradient Boosting. at <https://cran.r-project.org/web/packages/xgboost/> (2019).
22. Available Models | The caret Package. at <http://topepo.github.io/caret/available-models.html>.
23. Fernández-Delgado, M., Cernadas, E., Barro, S., Amorim, D., Fernández-Delgado, A. Do we Need Hundreds of Classifiers to Solve Real World Classification Problems? *Journal of Machine Learning Research*. **15**, 3133-3181 (2014).
24. Hira, Z. M., Gillies, D. F. A Review of Feature Selection and Feature Extraction Methods Applied on Microarray Data. *Advances in Bioinformatics*. **2015**, 198363 (2015).
25. Sánchez-Maroño, N., Alonso-Betanzos, A., Tombilla-Sanromán, M. Filter methods for feature selection - A comparative study. *Lecture Notes in Computer Science (including subseries Lecture Notes in Artificial Intelligence and Lecture Notes in Bioinformatics)*. **4881 LNCS**, 178–187, (2007).
26. Cawley, G.C., Talbot, N.L.C.C. Fast exact leave-one-out cross-validation of sparse least-squares support vector machines. *Neural Network.* **17** (10), 1467–1475 (2004).
27. Forghani, R. et al. Radiomics and Artificial Intelligence for Biomarker and Prediction Model Development in Oncology. *Computational and Structural Biotechnology Journal*. **17**, 995–1008 (2019).
28. Jaffe, C. C. Measures of response: RECIST, WHO, and new alternatives. *Journal of Clinical Oncology : Official Journal of the American Society of Clinical Oncology*. **24** (20), 3245–3251 (2006).
29. Lambin, P. et al. Radiomics: Extracting more information from medical images using advanced feature analysis. *European Journal of Cancer*. **48** (4), 441–446 (2012).
30. Gillies, R. J., Kinahan, P. E., Hricak, H. Radiomics: Images are more than pictures, they are

573 data. *Radiology*. **278** (2), 563–577 (2016).
574 31. Nioche, C. et al. Lifex: A freeware for radiomic feature calculation in multimodality
575 imaging to accelerate advances in the characterization of tumor heterogeneity. *Cancer Research*.
576 **78** (16), 4786–4789 (2018).
577 32. Ellmann, S. et al. Application of machine learning algorithms for multiparametric MRI-
578 based evaluation of murine colitis. *PLOS ONE*. **13** (10), e0206576 (2018).
579

Figure 1

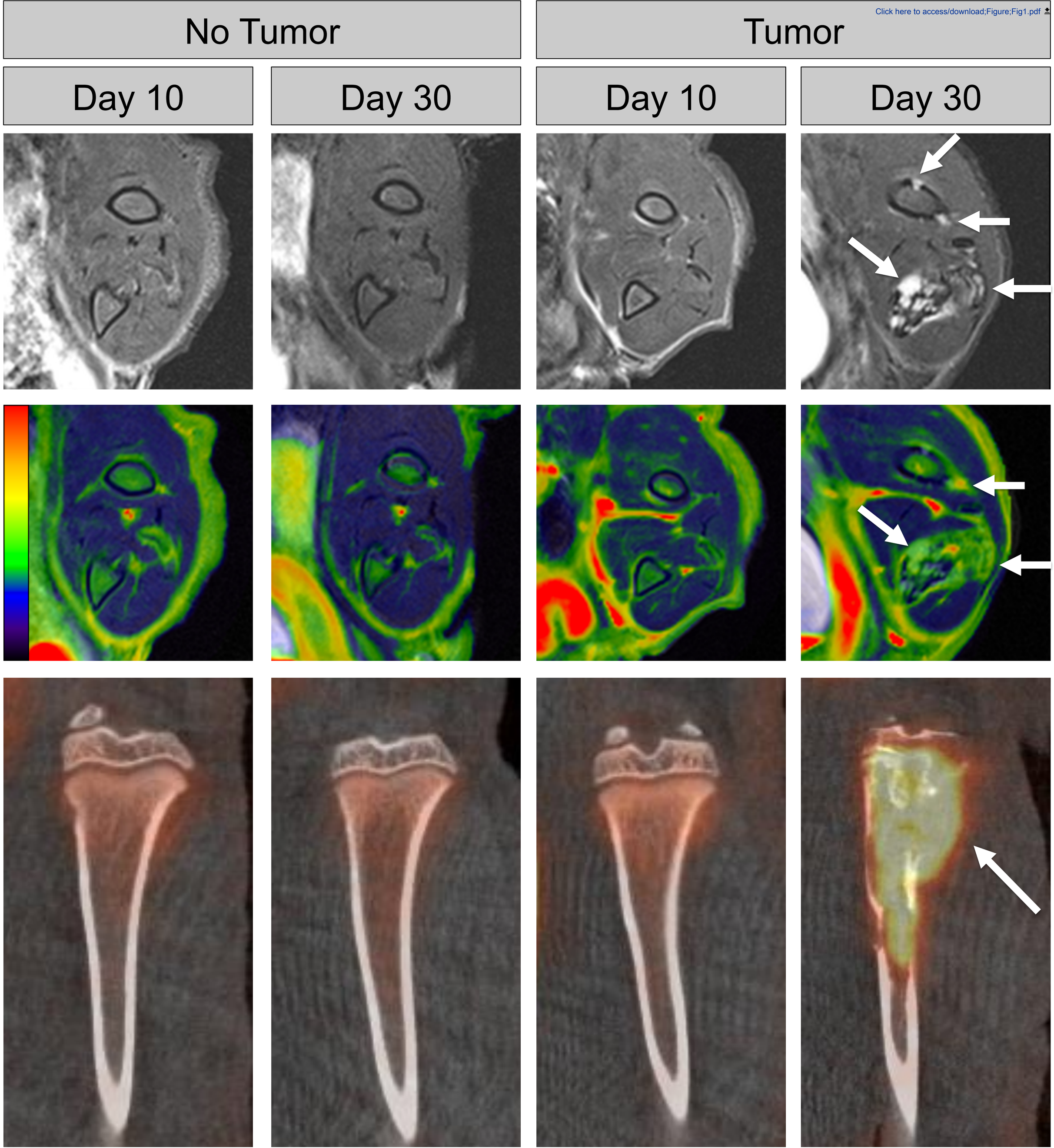

Figure 2

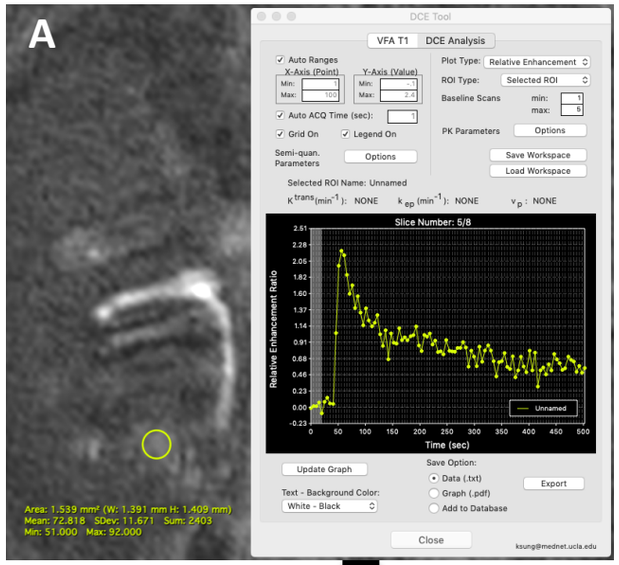

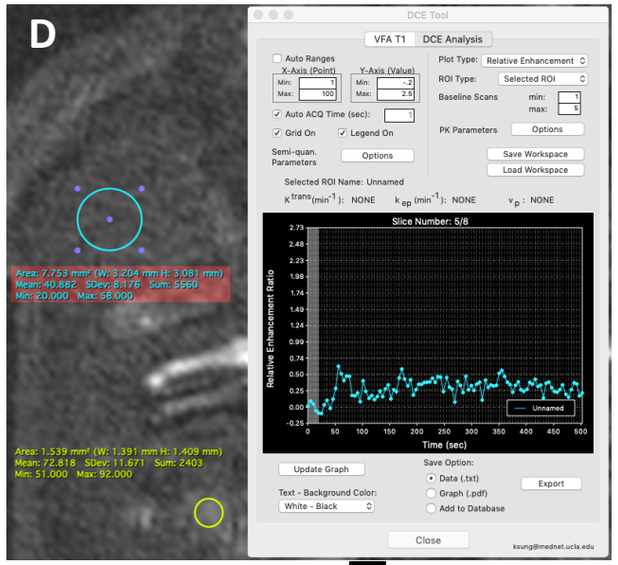

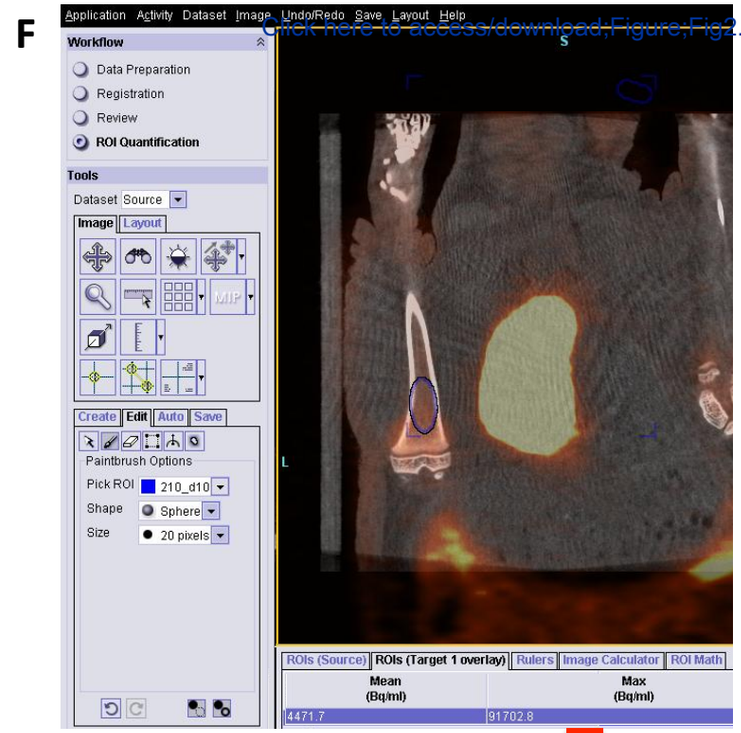

B

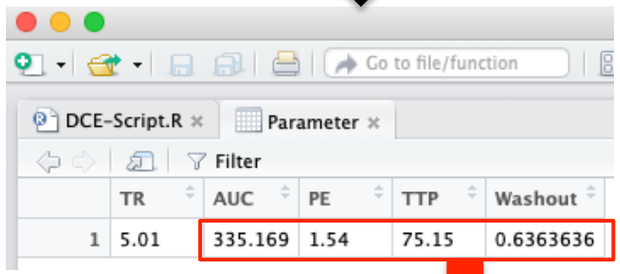

E

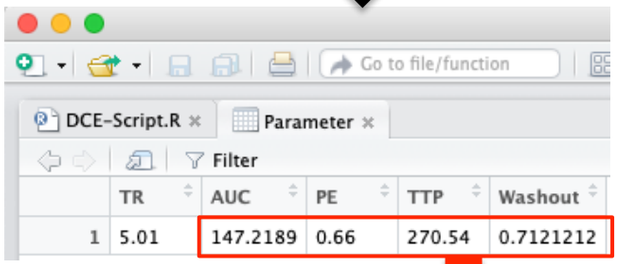

: Activity [Bq] × body weight [g]

C

	A	B	C	D	E	F	G	H	I	J	K	L	M	N	O
1	Animal#	Bone				Muscle				Normalized				PET	Tumor
2		AUC	PE	TTP	Washout	AUC	PE	TTP	Washout	AUC	PE	TTP	Washout	SUVmax	
3	1	335.169	1.54	75.15	0.63636364	147.21885	0.68	207.915	0.71759563	2.27667177	2.26470588	0.36144578	0.88679977	2.46047	1
4	2	350.9	1.705	70	0.74268503	138	0.5	155	0.45454545	2.54275362	3.41	0.4516129	1.63390706	2.70264	0
5	3	384.725	1.755	70	0.66231903	195.8	0.605	147.5	0.30306799	1.96488764	2.90082645	0.47457627	2.18538098	2.40002	1
6	4	264.025	1.52	65	0.75424463	166.7	0.615	135	0.68796791	1.58383323	2.47154472	0.48148148	1.09633693	2.51420	1
7	5	297.05	1.475	70	0.84083387	194.5	0.6	130	0.38392857	1.52724936	2.45833333	0.53846154	2.19007892	2.88922	0
8	6	374	1.735	70	0.67962815	165.1	0.525	180	0.43818182	2.26529376	3.3047619	0.38888889	1.5510186	2.09669	1
9	7	280.975	1.26	62.5	0.6495477	151.975	0.545	157.5	0.36849222	1.84882382	2.31192661	0.3968254	1.76271752	2.21714	1
10	8	301.725	1.75	62.5	0.65608466	161.075	0.53	162.5	0.29502327	1.87319572	3.30188679	0.38461538	2.22384035	2.82772	0
11	9	434.65	1.98	75	0.6074604	102	0.43	407.5	0.70594654	4.26127451	4.60465116	0.18404908	0.86049066	2.44902	0

Figure 3

Click here to access/download;Figure;Fig3.tiff

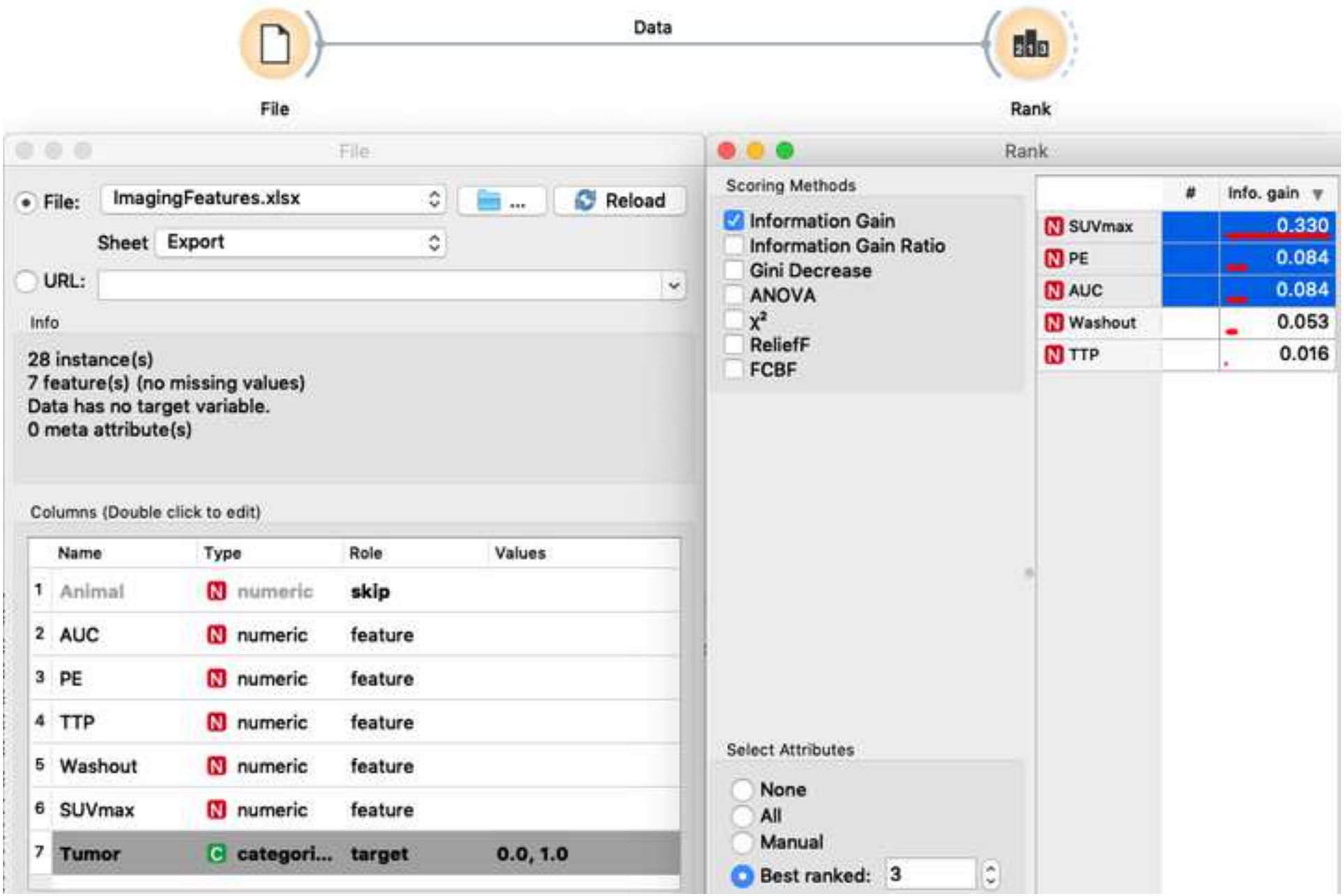

Figure 4

Click here to access/download;Figure;Fig4.pdf

A

```
Console ~/Downloads/
> Testmodel$bestTune
   size  decay   bag
12    3 0.0005 FALSE
> NeuralNetModel
Model Averaged Neural Network

28 samples
 3 predictor
 2 classes: 'X0', 'X1'

Pre-processing: Box-Cox transformation (3)
Resampling: Leave-One-Out Cross-Validation
Summary of sample sizes: 27, 27, 27, 27, 27, 27, ...
Resampling results:
```

B

```
  Accuracy   Kappa
  0.8571429  0.7021277

Tuning parameter 'size' was held constant at a value of 3
Tuning parameter 'decay' was held constant at a value
 of 0.0005
Tuning parameter 'bag' was held constant at a value of FALSE
> epi.tests(rev(epitable$table), conf.level = 0.95)
             Disease positive Disease negative Total
Test positive               15                1    16
Test negative                3                9    12
Total                       18               10    28
```

C

```
 Point estimates and 95 % CIs:
-----------------------------------------------------------
                                 Estimation Lower CI Upper CI
Apparent prevalence                   0.571    0.372    0.755
True prevalence                       0.643    0.441    0.814
Sensitivity                           0.833    0.586    0.964
Specificity                           0.900    0.555    0.997
Positive predictive value             0.938    0.698    0.998
Negative predictive value             0.750    0.428    0.945
Diagnstic accuracy                    0.857    0.673    0.960
Likelihood ratio of a positive test   8.333    1.283   54.114
Likelihood ratio of a negative test   0.185    0.065    0.531
-----------------------------------------------------------
>
> plot(roc.obj, print.auc=T)
```

D

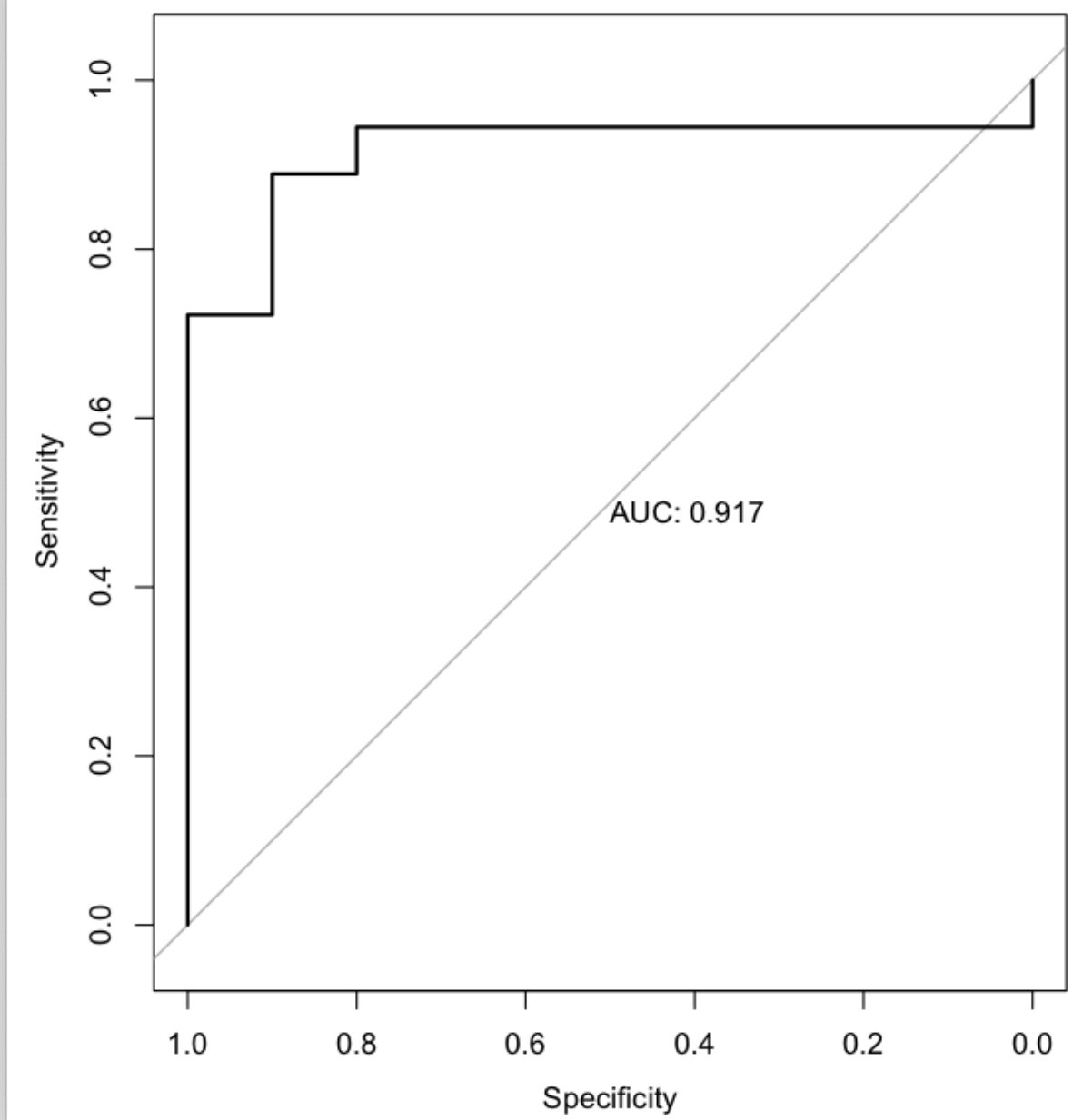

Table of Materials

Name of Material/ Equipment	Company	Catalog Number	Comments/Description
Binocular Operating Microscope	Leica	NA	
ClinScan MR System	Bruker	NA	
DICOM Viewer	Horos	NA	www.horosproject.org
Excel: Spreadsheet	Microsoft	NA	
FCS	Sigma	F2442-500ML	
Gadovist	Bayer-Schering	NA	
Inveon PET/CT	Siemens	NA	
Inveon Research Workplace Software	Siemens Healthcare GmbH	NA	
IVIS Spectrum	PerkinElmer	NA	
MDA-MB-231 human breast cancer cells	American Type Culture Collection	N/A	
Open-source data visualization, machine learning and data mining toolkit.	Orange3, University of Ljubljana	NA	https://orange.biolab.si/
RPMI-1640	Invitrogen/ThermoFisher	11875093	
Trypsin	Sigma	9002-07-7	
Vevo 3100	VisualSonics	NA	

Dear Dr. Heppenheimer,
Dear Editorial Office Team,
Dear Reviewers,

Thank you very much for your time and efforts regarding the revision of our manuscript (JoVE 61235). We appreciate the chance to further improve our paper. Please see the issues raised by the Editor and the reviewers in a point-by-point analysis below, along with our answers.
We hope to fulfill all requirements for publication in JoVE with the revised version of our manuscript.

Kind regards
Prof. Dr. Tobias Bäuerle, Corresponding author
Dr. Stephan Ellmann, First author.

Editorial comments:
Changes to be made by the Author(s):

1. Please take this opportunity to thoroughly proofread the manuscript to ensure that there are no spelling or grammar issues. The JoVE editor will not copy-edit your manuscript and any errors in the submitted revision may be present in the published version.

   Thank you for mentioning this issue. We performed a thorough proofread. Please be aware that many expressions might look awkward at first glance, such as "trainControl", "avNNet", "BoxCox". These are expressions used within RStudio for Machine Learning purposes. The awkward capitalization of these expressions is correct.

2. Please ensure that the Abstract is between 150-300 words.

   Thank you, we ensured that the word count of the abstract is exactly 300.

3. JoVE cannot publish manuscripts containing commercial language. Please remove all commercial language from your manuscript and use generic terms instead. All commercial products should be sufficiently referenced in the Table of Materials and Reagents.
   For example: Invitrogen, Germany, Sigma, Taufkirchen, Germany, Bruker ClinScan, Siemens, Germany, Bruker, Erlangen, Germany, Gadovist, Bayer-

Schering, Germany, Siemens Inveon, IVIS Spectrum, PerkinElmer, Vevo 3100, VisualSonics, Microsoft Excel, Horos, etc

We removed all commercial language from the manuscript and extended the Table of Materials and Reagents to now list these terms in detail. However, the term "RStudio" still shows up within the manuscript. This, however, is of great importance, as all the code provided is specific RStudio code. Although it is of no particular relevance which spreadsheet software or MRI scanner has been used, the presented code is highly specific for RStudio, so that we feel this software should be explicitly mentioned within the manuscript. Moreover, RStudio is non-commercial.

4. Please include an ethics statement before your numbered protocol steps, indicating that the protocol follows the animal care guidelines of your institution.

   We added a respective statement in lines 101–103.

5. Unfortunately, there are a few sections of the manuscript that show significant overlap with previously published work. Though there may be a limited number of ways to describe a technique, please use original language throughout the manuscript. Please see lines: 106-137, 143-160.

   We modified the respective paragraphs.

6. Please include a single line space between each step, substep and note in the protocol section.

   We included the requested spacing.

7. Please ensure that all text in the protocol section is written in the imperative tense as if telling someone how to do the technique (e.g., "Do this," "Ensure that," etc.). The actions should be described in the imperative tense in complete sentences wherever possible. Avoid usage of phrases such as "could be," "should be," and "would be" throughout the Protocol. Any text that cannot be written in the imperative tense may be added as a "Note."

   We modified the protocol section, which is now containing imperatives in complete sentences. We avoided the above-mentioned expressions.

8. The Protocol should be made up almost entirely of discrete steps without large paragraphs of text between sections. Please ensure that individual steps of the protocol should only contain 2-3 actions per step.

    We removed the respective text paragraphs between the protocol steps.
    We moreover tried to sufficiently shorten the individual sub-steps. However, with respect to the suggestion #10 ("Please add more details to your protocol steps") we unfortunately were only able to cut the sub-steps down to a maximum number of 5 sub-steps.
    To further streamline the structure of our manuscript, we divided the Machine Learning part of the protocol into 3 separate steps: 1) Preparation; 2) Machine Learning; 3) Analysis of the results.
    We sincerely hope to fulfill the Editorial Office's request with this approach.

9. Please revise the protocol text to avoid the use of any personal pronouns in the protocol (e.g., "we", "you", "our" etc.).

    The protocol has been revised accordingly.

10. Please add more details to your protocol steps. Please ensure you answer the "how" question, i.e., how is the step performed? Please include all the button clicks, knob turns, command lines etc.

    Thank you for raising this issue. Regarding the command lines, we provide in-depth code excerpts of all steps. We moreover included the Script files as supplementary, so that the user will not have to type in the commands by hand. Moreover, most of the code executions will also be shown within the video. We believe that a standard computer user will be capable of following the steps.
    We moreover added terms such as "Click on", "Select", … where appropriate.

11. 1.5: How do you check the depth of anesthesia?

    We checked the depth of anesthesia by toe pinching. We added this step to the protocol.

12. 2, 3, 4: Please include how each step is performed. Please include button clicks, knob turns etc. Alternatively include references.

    We share the Editorial Office's point that imaging is a complex task. However, we felt that this protocol should rather focus on the application of machine learning algorithms, and not on the details to operate an MRI or PET/CT machine. Therefore, we think that describing complex imaging procedures in detail would be beyond the scope of this JoVE article. The information given on the imaging procedures in brief aims to provide the reader with crucial aspects such as sequence types for the MRI. For further information on imaging procedures, we have referenced to relevant publications containing these data in more detail.

13. 5,6, 7: Please use your example experiment and describe these steps accordingly. For the software steps please ensure all the steps are described providing all specific details. E.g., How did you load the MRI images in software? What is the region of interest in your experiment? How did you adjust the baseline scans? Where did you export the files to? Please include all the details for 6 and 7 as well.

    The steps of analyzing the acquired images, analyzing the data and programming the Machine Learning algorithm have been modified and now present the required steps in greater detail.

14. There is a 10-page limit for the Protocol, but there is a 2.75-page limit for filmable content. Please highlight 2.75 pages or less of the Protocol (including headings and spacing) that identifies the essential steps of the protocol for the video, i.e., the steps that should be visualized to tell the most cohesive story of the Protocol.

    We cut down the parts of the manuscript highlighted in yellow to approximately 3 pages. This was achieved by deleting some parts of the code, as the code is provided within the supplementary files anyway. It would be easily possible to cut the yellow-marked paragraphs to well below 2.75 pages by deleting all the code and consequently refer to the supplementary files. However, as the code represents the pivotal substance of our manuscript, we suggest to include the given information. To our understanding, the video will show the execution of the code anyway, regardless of the yellow highlighting within the

manuscript. Please let us know if JoVE can make an exception for this IT-based article. Otherwise, we can delete all the code to remain within the 2.75 pages limit and refer to the supplementary files in all respective paragraphs.

15. Please describe the result with respect to your experiment, you performed an experiment, how did it help you to conclude what you wanted to, how is it in line with the title, how do these results show the technique, suggestions about how to analyze the outcome, etc Please include all your observation in the form of figures/table and what did you conclude from this study.

    We added three different paragraphs to the Representative Results: Positive Results, Negative Results, and "What could go wrong".
    The positive results conclude that combining the parameters to an avNNet significantly increases accuracy (also compare Reviewer #1, Major issue #2).
    The negative results paragraph describes what can be observed when choosing suboptimal algorithms or deciding to skip preprocessing.
    The "What could go wrong" section points out difficulties when changing the manuscript to fit other purposes.

16. As we are a methods journal, please revise the Discussion to explicitly cover the following in detail in 3-6 paragraphs with citations:
    a) Critical steps within the protocol
    b) Any modifications and troubleshooting of the technique
    c) Any limitations of the technique
    d) The significance with respect to existing methods
    e) Any future applications of the technique

    We adapted the discussion. Critical steps and modifications are presented within paragraph 1 and 2 of the discussion.
    Future applications and suggestions for improvement and modifications for different problems are presented in the second part of the last paragraph.

Reviewers' comments:
Reviewer #1:
Manuscript Summary:

The authors demonstrated an exciting way by applying the avNNet model for the detection of bone metastases in the rate model. The top features of avNNET model were extracted based on the output from the Orange3 feature ranking analysis. Then, the authors used these features to train avNNet mode, further tuned the model through a hyperparameter search. The performance metric for the avNNET model was provided with high accuracy. The authors conclude that the applicability of the model is transferable to other fields of study. However, there are several comments/concerns which are provide below.

Major Concerns:

1. The top features were extracted using the Orange3 analysis. How does it rank the features?

> *Thank you for raising the important issue of feature selection. We already provide more in-depth information on this issue within the revised version of your manuscript, including the protocol steps and the use of the "Information Gain" method to rank features. We additionally cited a publication on this topic in the protocol and in the discussion (DOI: 10.1093/bioinformatics/btm344).*

2. If the Orange3 is capable of extracting the key features, what is the major value-add of the proposed avNNET model to the scientific community?

> *This is another important issue and we want to thank the reviewer for giving us the chance to clarify this point. Combining relevant features to an avNNet drastically increases the prediction accuracy, so that the model's accuracy significantly exceeds the accuracies of all its constituents. To prove this fact, we added a step within the protocol (#12), in which the model's ROC curve is compared to the ROC curves of its constituents. The model proved to perform significantly better (all, $p \leq 0.01$).*

3. The sample size is 27, which is extremely small for the Neural Net models. How would the authors ensure the avNNET model is not suffering from overfitting?

> *The sample size in our protocol is 28. However, the reviewer is absolutely correct that this is quite a small sample size for the purpose of machine learning. Ideally, one would randomly remove a fraction of animals from the entire data set and treat them as a test set, while training the avNNet on the remainder of the animals to subsequently*

predict the outcome of the test set. This procedure would, however, need considerably higher numbers of animals. To create a generalizable model and prevent overfitting, a leave-one-out cross validation was used in this study. We extended the discussion on this issue.

Minor Concerns:
1. A sample DCE file is missing in the supplementary section. Without it, it is hard to validate the code/results.

We added a sample DCE file named "DCEraw.txt". We changed the protocol, so that the file name for the DCE raw data is now "DCEraw.txt" (formerly: "Untitled.txt").

2. Several typo were found on the doc.

Thank you for mentioning this issue. We performed a thorough proofread of the revised version of our manuscript.

Reviewer #2:

Manuscript Summary:

The paper describes an interesting protocol that can have a sensible impact in many areas of oncology for early time point detection when macroscopic changes within the bone are not yet visually perceivable.

Major Concerns:

Image processing methods and AVnet needs to be better introduced by providing a high level presentation of the methodologies prior to entering their detailed step-by-step usage.

> *Thank you for mentioning this weakness. We added more information to the end of the introduction, just prior to entering the protocol.*

Minor Concerns:

I would suggest avoiding the use of commercial sw such as excel when many open source alternatives do exist.

> *Thank you for raising this issue. Indeed, the use of MS Excel is not crucial and we omitted this term from the manuscript. The other software packages, including Horos, Orange, RStudio, and the caret package, are open source/freeware products.*

ELSEVIER LICENSE
TERMS AND CONDITIONS

Jan 08, 2020

This Agreement between Stephan Ellmann ("You") and Elsevier ("Elsevier") consists of your license details and the terms and conditions provided by Elsevier and Copyright Clearance Center.

License Number	4744270680316
License date	Jan 08, 2020
Licensed Content Publisher	Elsevier
Licensed Content Publication	Bone
Licensed Content Title	Prediction of early metastatic disease in experimental breast cancer bone metastasis by combining PET/CT and MRI parameters to a Model-Averaged Neural Network
Licensed Content Author	Stephan Ellmann,Lisa Seyler,Jochen Evers,Henrik Heinen,Aline Bozec,Olaf Prante,Torsten Kuwert,Michael Uder,Tobias Bäuerle
Licensed Content Date	Mar 1, 2019
Licensed Content Volume	120
Licensed Content Issue	n/a
Licensed Content Pages	8
Start Page	254
End Page	261
Type of Use	reuse in a journal/magazine

Requestor type	academic/educational institute
Portion	figures/tables/illustrations
Number of figures/tables/illustrations	1
Format	both print and electronic
Are you the author of this Elsevier article?	Yes
Will you be translating?	No
Title of new article	Machine learning algorithms for early detection of bone metastases in an experimental rat model
Lead author	Stephan Ellmann, MD
Title of targeted journal	Journal of Visualized Experiments (JoVE)
Publisher	MyJove Corp.
Expected publication date	Apr 2020
Portions	Fig. 1
Requestor Location	Stephan Ellmann Radiologisches Institut Maximiliansplatz 1 Erlangen, 91054 Germany Attn: Stephan Ellmann
Publisher Tax ID	GB 494 6272 12
Total	0.00 EUR

Terms and Conditions

INTRODUCTION

1. The publisher for this copyrighted material is Elsevier. By clicking "accept" in connection with completing this licensing transaction, you agree that the following terms and conditions apply to this transaction (along with the Billing and Payment terms and conditions established by Copyright Clearance Center, Inc. ("CCC"), at the time that you opened your Rightslink account and that are available at any time at http://myaccount.copyright.com).

GENERAL TERMS

2. Elsevier hereby grants you permission to reproduce the aforementioned material subject to the terms and conditions indicated.

3. Acknowledgement: If any part of the material to be used (for example, figures) has appeared in our publication with credit or acknowledgement to another source, permission must also be sought from that source. If such permission is not obtained then that material may not be included in your publication/copies. Suitable acknowledgement to the source must be made, either as a footnote or in a reference list at the end of your publication, as follows:

"Reprinted from Publication title, Vol /edition number, Author(s), Title of article / title of chapter, Pages No., Copyright (Year), with permission from Elsevier [OR APPLICABLE SOCIETY COPYRIGHT OWNER]." Also Lancet special credit - "Reprinted from The Lancet, Vol. number, Author(s), Title of article, Pages No., Copyright (Year), with permission from Elsevier."

4. Reproduction of this material is confined to the purpose and/or media for which permission is hereby given.

5. Altering/Modifying Material: Not Permitted. However figures and illustrations may be altered/adapted minimally to serve your work. Any other abbreviations, additions, deletions and/or any other alterations shall be made only with prior written authorization of Elsevier Ltd. (Please contact Elsevier at permissions@elsevier.com). No modifications can be made to any Lancet figures/tables and they must be reproduced in full.

6. If the permission fee for the requested use of our material is waived in this instance, please be advised that your future requests for Elsevier materials may attract a fee.

7. Reservation of Rights: Publisher reserves all rights not specifically granted in the combination of (i) the license details provided by you and accepted in the course of this licensing transaction, (ii) these terms and conditions and (iii) CCC's Billing and Payment terms and conditions.

8. License Contingent Upon Payment: While you may exercise the rights licensed immediately upon issuance of the license at the end of the licensing process for the transaction, provided that you have disclosed complete and accurate details of your proposed use, no license is finally effective unless and until full payment is received from you (either by publisher or by CCC) as provided in CCC's Billing and Payment terms and conditions. If full payment is not received on a timely basis, then any license preliminarily granted shall be deemed automatically revoked and shall be void as if never granted. Further, in the event that you breach any of these terms and conditions or any of CCC's Billing and Payment terms and conditions, the license is automatically revoked and shall be void as if never granted. Use of materials as described in a revoked license, as well as any use of the materials beyond the scope of an unrevoked license, may constitute copyright infringement and publisher reserves the right to take any and all action to protect its copyright in the materials.

9. Warranties: Publisher makes no representations or warranties with respect to the licensed material.

10. Indemnity: You hereby indemnify and agree to hold harmless publisher and CCC, and their respective officers, directors, employees and agents, from and against any and all claims arising out of your use of the licensed material other than as specifically authorized pursuant to this license.

11. No Transfer of License: This license is personal to you and may not be sublicensed, assigned, or transferred by you to any other person without publisher's written permission.

12. No Amendment Except in Writing: This license may not be amended except in a writing signed by both parties (or, in the case of publisher, by CCC on publisher's behalf).

13. Objection to Contrary Terms: Publisher hereby objects to any terms contained in any purchase order, acknowledgment, check endorsement or other writing prepared by you, which terms are inconsistent with these terms and conditions or CCC's Billing and Payment terms and conditions. These terms and conditions, together with CCC's Billing and Payment terms and conditions (which are incorporated herein), comprise the entire agreement between you and publisher (and CCC) concerning this licensing transaction. In the event of any conflict between your obligations established by these terms and conditions and those established by CCC's Billing and Payment terms and conditions, these terms and conditions shall control.

14. Revocation: Elsevier or Copyright Clearance Center may deny the permissions described in this License at their sole discretion, for any reason or no reason, with a full refund payable to you. Notice of such denial will be made using the contact information provided by you. Failure to receive such notice will not alter or invalidate the denial. In no event will Elsevier or Copyright Clearance Center be responsible or liable for any costs, expenses or damage incurred by you as a result of a denial of your permission request, other than a refund of the amount(s) paid by you to Elsevier and/or Copyright Clearance Center for denied permissions.

LIMITED LICENSE

The following terms and conditions apply only to specific license types:

15. **Translation**: This permission is granted for non-exclusive world **English** rights only unless your license was granted for translation rights. If you licensed translation rights you may only translate this content into the languages you requested. A professional translator must perform all translations and reproduce the content word for word preserving the integrity of the article.

16. **Posting licensed content on any Website**: The following terms and conditions apply as follows: Licensing material from an Elsevier journal: All content posted to the web site must maintain the copyright information line on the bottom of each image; A hyper-text must be included to the Homepage of the journal from which you are licensing at http://www.sciencedirect.com/science/journal/xxxxx or the Elsevier homepage for books at http://www.elsevier.com; Central Storage: This license does not include permission for a scanned version of the material to be stored in a central repository such as that provided by Heron/XanEdu.

Licensing material from an Elsevier book: A hyper-text link must be included to the Elsevier homepage at http://www.elsevier.com . All content posted to the web site must maintain the copyright information line on the bottom of each image.

Posting licensed content on Electronic reserve: In addition to the above the following clauses are applicable: The web site must be password-protected and made available only to

bona fide students registered on a relevant course. This permission is granted for 1 year only. You may obtain a new license for future website posting.

17. **For journal authors:** the following clauses are applicable in addition to the above:

Preprints:

A preprint is an author's own write-up of research results and analysis, it has not been peer-reviewed, nor has it had any other value added to it by a publisher (such as formatting, copyright, technical enhancement etc.).

Authors can share their preprints anywhere at any time. Preprints should not be added to or enhanced in any way in order to appear more like, or to substitute for, the final versions of articles however authors can update their preprints on arXiv or RePEc with their Accepted Author Manuscript (see below).

If accepted for publication, we encourage authors to link from the preprint to their formal publication via its DOI. Millions of researchers have access to the formal publications on ScienceDirect, and so links will help users to find, access, cite and use the best available version. Please note that Cell Press, The Lancet and some society-owned have different preprint policies. Information on these policies is available on the journal homepage.

Accepted Author Manuscripts: An accepted author manuscript is the manuscript of an article that has been accepted for publication and which typically includes author-incorporated changes suggested during submission, peer review and editor-author communications.

Authors can share their accepted author manuscript:

- immediately
    - via their non-commercial person homepage or blog
    - by updating a preprint in arXiv or RePEc with the accepted manuscript
    - via their research institute or institutional repository for internal institutional uses or as part of an invitation-only research collaboration work-group
    - directly by providing copies to their students or to research collaborators for their personal use
    - for private scholarly sharing as part of an invitation-only work group on commercial sites with which Elsevier has an agreement
- After the embargo period
    - via non-commercial hosting platforms such as their institutional repository
    - via commercial sites with which Elsevier has an agreement

In all cases accepted manuscripts should:

- link to the formal publication via its DOI
- bear a CC-BY-NC-ND license - this is easy to do
- if aggregated with other manuscripts, for example in a repository or other site, be shared in alignment with our hosting policy not be added to or enhanced in any way to appear more like, or to substitute for, the published journal article.

Published journal article (JPA): A published journal article (PJA) is the definitive final record of published research that appears or will appear in the journal and embodies all value-adding publishing activities including peer review co-ordination, copy-editing, formatting, (if relevant) pagination and online enrichment.

Policies for sharing publishing journal articles differ for subscription and gold open access articles:

Subscription Articles: If you are an author, please share a link to your article rather than the full-text. Millions of researchers have access to the formal publications on ScienceDirect, and so links will help your users to find, access, cite, and use the best available version.

Theses and dissertations which contain embedded PJAs as part of the formal submission can be posted publicly by the awarding institution with DOI links back to the formal publications on ScienceDirect.

If you are affiliated with a library that subscribes to ScienceDirect you have additional private sharing rights for others' research accessed under that agreement. This includes use for classroom teaching and internal training at the institution (including use in course packs and courseware programs), and inclusion of the article for grant funding purposes.

Gold Open Access Articles: May be shared according to the author-selected end-user license and should contain a CrossMark logo, the end user license, and a DOI link to the formal publication on ScienceDirect.

Please refer to Elsevier's posting policy for further information.

18. **For book authors** the following clauses are applicable in addition to the above: Authors are permitted to place a brief summary of their work online only. You are not allowed to download and post the published electronic version of your chapter, nor may you scan the printed edition to create an electronic version. **Posting to a repository:** Authors are permitted to post a summary of their chapter only in their institution's repository.

19. **Thesis/Dissertation**: If your license is for use in a thesis/dissertation your thesis may be submitted to your institution in either print or electronic form. Should your thesis be published commercially, please reapply for permission. These requirements include permission for the Library and Archives of Canada to supply single copies, on demand, of the complete thesis and include permission for Proquest/UMI to supply single copies, on demand, of the complete thesis. Should your thesis be published commercially, please reapply for permission. Theses and dissertations which contain embedded PJAs as part of the formal submission can be posted publicly by the awarding institution with DOI links back to the formal publications on ScienceDirect.

Elsevier Open Access Terms and Conditions

You can publish open access with Elsevier in hundreds of open access journals or in nearly 2000 established subscription journals that support open access publishing. Permitted third party re-use of these open access articles is defined by the author's choice of Creative Commons user license. See our open access license policy for more information.

Terms & Conditions applicable to all Open Access articles published with Elsevier:

Any reuse of the article must not represent the author as endorsing the adaptation of the article nor should the article be modified in such a way as to damage the author's honour or reputation. If any changes have been made, such changes must be clearly indicated.

The author(s) must be appropriately credited and we ask that you include the end user license and a DOI link to the formal publication on ScienceDirect.

If any part of the material to be used (for example, figures) has appeared in our publication with credit or acknowledgement to another source it is the responsibility of the user to ensure their reuse complies with the terms and conditions determined by the rights holder.

Additional Terms & Conditions applicable to each Creative Commons user license:

CC BY: The CC-BY license allows users to copy, to create extracts, abstracts and new works from the Article, to alter and revise the Article and to make commercial use of the Article (including reuse and/or resale of the Article by commercial entities), provided the user gives appropriate credit (with a link to the formal publication through the relevant DOI), provides a link to the license, indicates if changes were made and the licensor is not represented as endorsing the use made of the work. The full details of the license are available at http://creativecommons.org/licenses/by/4.0.

CC BY NC SA: The CC BY-NC-SA license allows users to copy, to create extracts, abstracts and new works from the Article, to alter and revise the Article, provided this is not done for commercial purposes, and that the user gives appropriate credit (with a link to the formal publication through the relevant DOI), provides a link to the license, indicates if changes were made and the licensor is not represented as endorsing the use made of the work. Further, any new works must be made available on the same conditions. The full details of the license are available at http://creativecommons.org/licenses/by-nc-sa/4.0.

CC BY NC ND: The CC BY-NC-ND license allows users to copy and distribute the Article, provided this is not done for commercial purposes and further does not permit distribution of the Article if it is changed or edited in any way, and provided the user gives appropriate credit (with a link to the formal publication through the relevant DOI), provides a link to the license, and that the licensor is not represented as endorsing the use made of the work. The full details of the license are available at http://creativecommons.org/licenses/by-nc-nd/4.0. Any commercial reuse of Open Access articles published with a CC BY NC SA or CC BY NC ND license requires permission from Elsevier and will be subject to a fee.

Commercial reuse includes:

- Associating advertising with the full text of the Article
- Charging fees for document delivery or access
- Article aggregation
- Systematic distribution via e-mail lists or share buttons

Posting or linking by commercial companies for use by customers of those companies.

20. **Other Conditions**:

v1.9

Questions? customercare@copyright.com or +1-855-239-3415 (toll free in the US) or +1-978-646-2777.

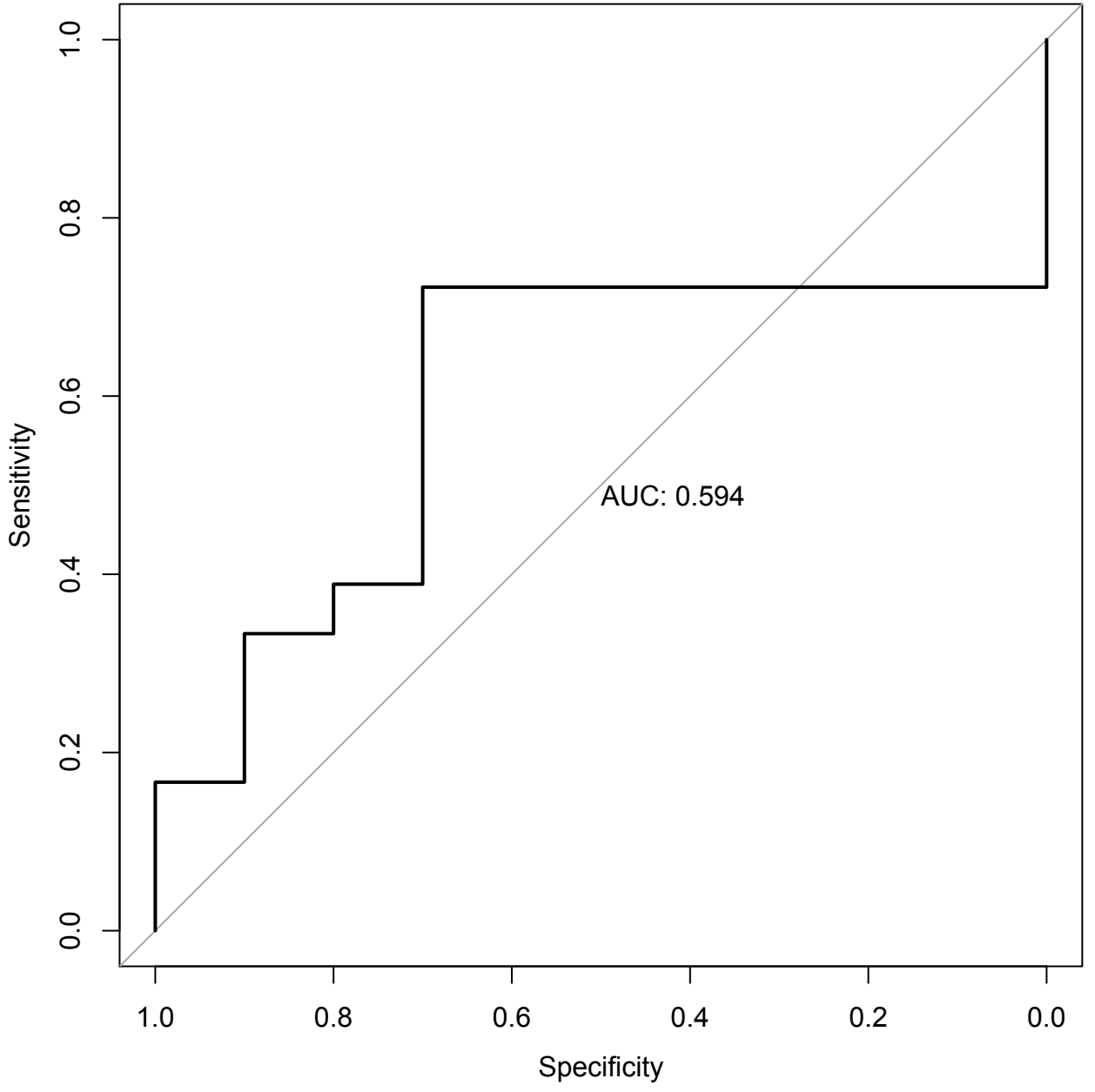

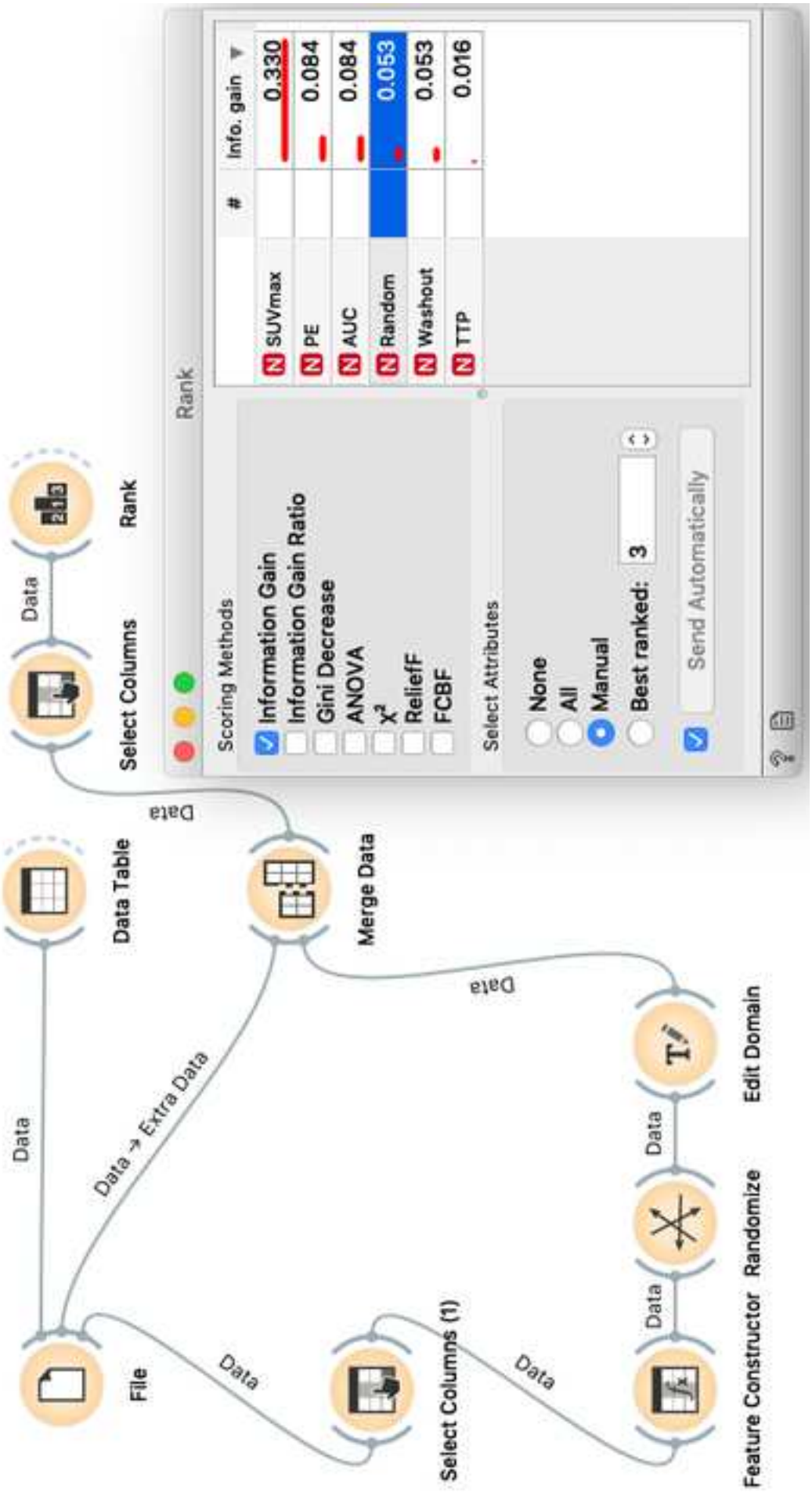

Excel Sheet

Click here to access/download

Supplemental Coding Files

ImagingFeatures.xlsx

DCE analysis R Script

Exemplary DCE raw measurements

Machine Learning Script